Composite Structures 133 (2015) 642–651

Contents lists available at ScienceDirect

Composite Structures

journal homepage: www.elsevier.com/locate/compstruct

Design and analysis of smart release devices based on shape memory polymer composites

Hanqing Wei [a], Liwu Liu [b], Zhichun Zhang [a], Haiyang Du [b], Yanju Liu [b], Jinsong Leng [a,*]

[a] Centre for Composite Materials and Structure, Science Park of Harbin Institute of Technology (HIT), P.O. Box 3011, No. 2 YiKuang Street, Harbin 150080, People's Republic of China
[b] Department of Astronautical Science and Mechanics, Harbin Institute of Technology (HIT), P.O. Box 301, No. 92 West Dazhi Street, Harbin 150001, People's Republic of China

ARTICLE INFO

Article history:
Available online 23 July 2015

Keywords:
Release devices
Shape memory polymer composites
Carbon-fiber fabric
Deformation recovery

ABSTRACT

Pyrotechnic release devices of spacecraft produce high-shock and contamination, which are hazardous. Mechanical release devices can overcome these disadvantages, but they tend to be complex and costly. In this paper, new kinds of release devices (smart release devices) with the advantages of no pyrotechnic, light weight, and simple structure are proposed, which are made of carbon fiber reinforced styrene-based shape memory polymer composite. The key element of the devices is the shape memory polymer composite cylinder (thin-walled tube). First, the smart release devices are designed based on three different deformation ways of the cylinder. Second, the deformation models are analyzed to verify the feasibility of the smart release devices. Then the smart release devices are made according to the design, they agree well with the simulations obtained from ABAQUS. Finally, the tensile experiments were conducted to get the structural strength of the devices. Different forms of the deformation were tested and compared, obtained the release time of the devices.

1. Introduction

Traditional pyrotechnic release devices are widely used to accommodate separation from the launch vehicle and deployment of solar arrays and other appendages. But they cause unnecessary contamination and have costly handling requirements due to their hazardous nature [1]. The United States, Russia and other countries have used memory alloys as the material of release mechanism in space fields since 1980s [2,3,4]. The Fast Acting, Shock less Separation Nut, developed by Strays Research Corporation, represents a kind of release devices with low-shock and non-pyrotechnic [5]. However, it is relatively complex in design. The stockless Thermally Actuated Release Nut (Star Nut) was made of Elastic Memory Composite in 2003. The Star Nut was provided with tremendous potential for reduced mass, complexity and cost [6]. Although the Start Nut has proven to be an inherent simplified design alternative to FASSN, it did not get the deformation performance and the release time of the devices. This work represents a kind of release devices made of shape memory polymer composites.

Shape memory polymers (SMPs) are stiff like plastic in their glassy state. However, when they are heated above the transition temperature (*Tg*), they become soft and have large strain capability [7]. Further following a cooling process, they become stiff again [8,9]. Compared with other smart materials such as shape memory alloy, SMP possesses the advantages of large deformation capacity, low density and low cost [10]. However, their drawbacks are low actuation forces and long recovery time [11–14]. For the sake of their low stiffness and strength, shape memory polymer composites (SMPCs), which were filled with particles, carbon nano-tubes, and short fibers were investigated [15–20]. To date, SMPCs and their products such as deployable and morphing structures have been researched and developed, including robotics [21], antenna, beam and solar array in space [22–24]. Besides, they have obtained widely use in the smart materials and structures field and other applications [25–32].

The smart release devices in this work were made of the carbon-fiber fabric reinforced shape memory polymer composites. The key to achieve simplicity is same with the Star Nut, they both use of mechanically simple active element, viz. cylinders. But the SMPC cylinders in the smart release devices were designed and created based on different ways of deformation. The bending, twisting and shrinking recovery deformations were used to drive the release between the mating halves of the mechanism, so the

* Corresponding author. Tel./fax: +86 451 86402328.
E-mail address: lengjs@hit.edu.cn (J. Leng).

http://dx.doi.org/10.1016/j.compstruct.2015.07.107
0263-8223/

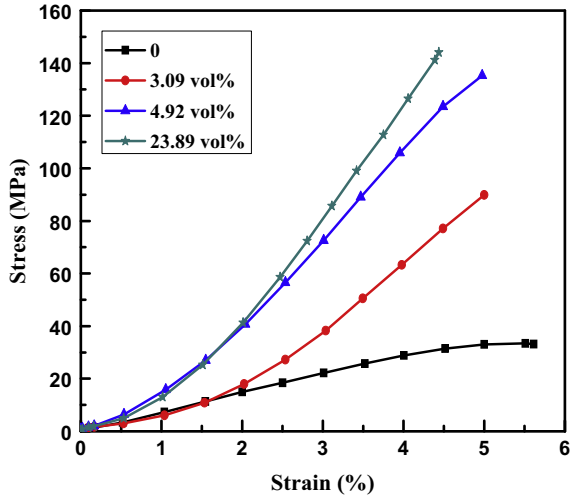

Fig. 1. Stress–strain relations of SMPCs incorporated with carbon-fiber fabric of different volume fractions at 25 °C.

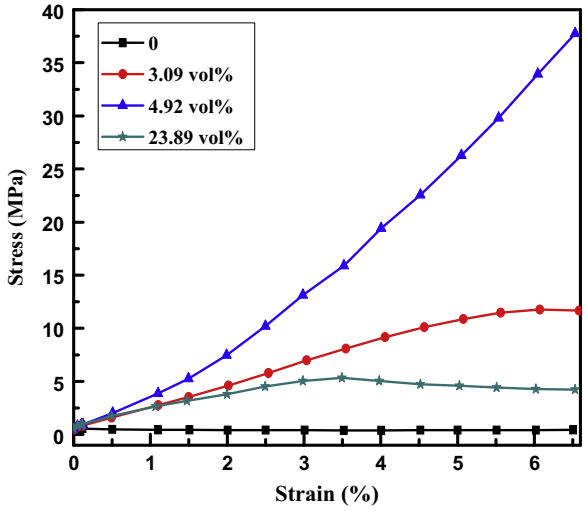

Fig. 2. Stress–strain relations of SMPCs incorporated with carbon-fiber fabric of different volume fractions at 90 °C.

corresponding smart release devices were named as "Lotus" device, "Eight paws" device and "Bamboo" device respectively. Their recovery performances were analyzed to confirm the release feasibility. Meanwhile, these smart release devices can finish release upon load with no impacting shock, space debris and contamination.

2. Materials

In this work, the materials are fabricated by the standard fabrication techniques for fiber reinforced composite. The SMP is same with reference [10] and the phase transition temperature of styrene is 67 °C. Carbon-fiber fabric (T300-3K, plain fabric) was spread on the glass template and the volume fractions are 3.09%, 4.92%, 23.89% respectively. For comparison, a pure SMP specimen was cured under the same conditions. Dumbbell specimens were prepared according to ASTM standard D638, the thickness of the SMPC specimen is around 2 mm.

From the tensile experiment of the materials at room temperature (25 °C), as shown in Fig. 1, the maximum stress of SMPC with 4.92% carbon-fiber is 137.25 MPa. It is about 4 times of the styrene. With the increasing of carbon-fiber fabric, modulus and strength increased and the strain decreased from 5.61% to 4.44%. Fig. 2 shows the stress of the SMPC decreased significantly at 90 °C and the styrene became soft. However, the maximum stress of 4.92% carbon fiber fabric reinforced styrene is 48.92 MPa, which is about

Table 1
Preliminary smart release devices requirements.

Description	Specification
Actuation time	<30 s
Temperature range	25–90 °C
Actuation power	15 W (min)

Table 2
Characteristics of the SMPC cylinders.

Characteristics	The inner cylinder (mm)	The outer cylinder (mm)
Long	110	70
The inner diameter	34	66
Thickness	2	2

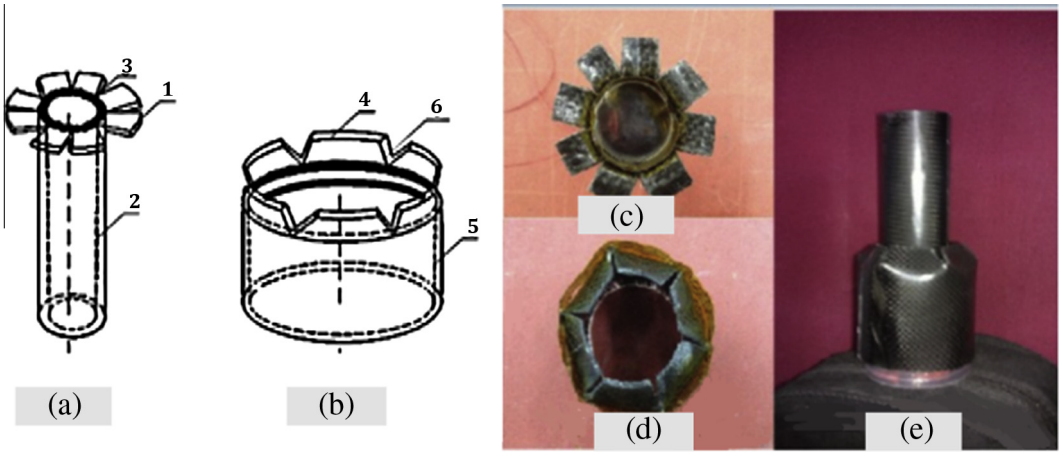

Fig. 3. (a) Design of the inner cylinder in the "Lotus" device. (b) Design of the outer cylinder in the "Lotus" device. (c) The inner cylinder in the "Lotus" device. (d) The outer cylinder in the "Lotus" device. (e) The "Lotus" device.

50 times of the styrene. So SMPC with 4.92% carbon-fiber fabric was selected as the main material of the smart release devices due to the identified high modulus and strength at 90 °C. Besides, it has good deformation in all the materials presented in Fig. 2.

3. Design and fabrication of the smart release devices

In the study, the smart release devices were designed, as shown in Table 1. The cylinders of the smart release devices were produced and the relevant characteristics are listed in Table 2.

The "Lotus" device consists of the inner and outer cylinders with different diameter; it uses the bending deformation as the driving deployment. Fig. 3(a) and (b) shows the parts of the "Lotus" device are: 1-eight arc-shaped deformable laminates, 2-inner cylinder, 3-resistor heater, 4-six trapezium-shaped deformable laminates, 5-outer cylinder and 6-resistor heater. The assembling process of the "Lotus" device is: On the one hand, one side of the inner cylinder was cut into eight arc-shaped deformable laminates, 13.5 mm in length. Then, the resistor heater was bonded on the inside surfaces of the inner cylinder, 13.5 mm in length. Finally, the other end of the inner cylinder was fixed on the shelf. On the other hand, one side of the outer cylinder was cut to form six trapezium-shaped deformable laminates with an angle of 60 degrees (°) to each other, 13.5 mm in length. Meanwhile, they formed a hole when they were bent to 60°, 38 mm in diameter. Then, the resistor heater was bonded on the

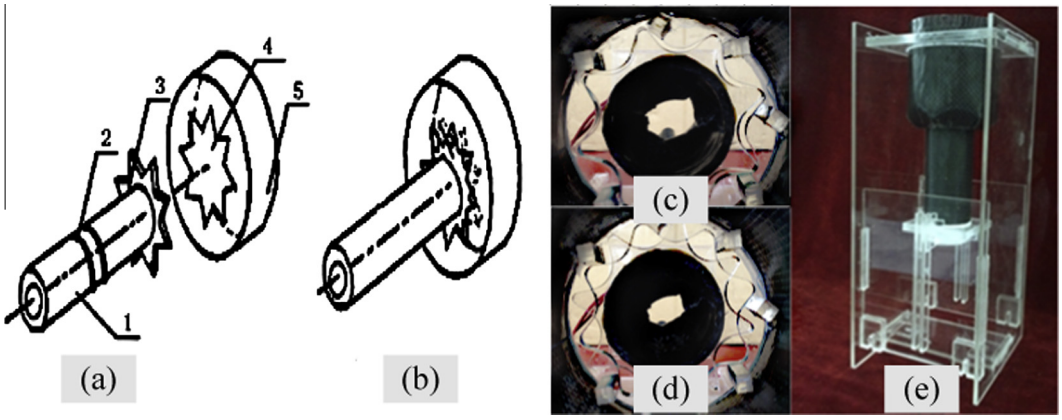

Fig. 4. (a) Design of the cylinders in the "Eight paws" device. (b) Design of the "Eight paws" device. (c) The release state of the "Eight paws" device. (d) The connection state of the "Eight paws" device. (e) The "Eight paws" device.

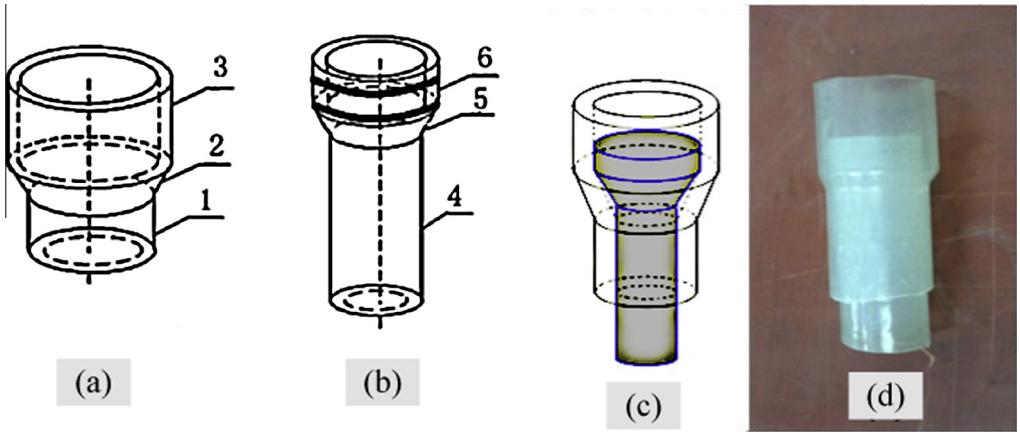

Fig. 5. (a) Design of the outer cylinder in the "Bamboo" device. (b) Design of the inner cylinder in the "Bamboo" device. (c) The connection state of the "Bamboo" device. (d) The "Bamboo" device.

Table 3
Material parameters of the SMPC.

Carbon fiber ratio (%)	Density (kg/m^3)	Modulus1 (MPa)	Modulus2 (MPa)	Elongation1 (%)	Elongation2 (%)
0	1.03	6.87	0.01	16.58	54.08
3.09	1.04	24.17	2.07	5.40	35.97
4.92	1.05	33.00	5.56	4.92	34.69
23.89	1.17	42.76	–	4.23	34.18

Note: Elongation 1 – elongation of the composites at 25 °C; Elongation 2 – elongation of the composites at 90 °C; Modulus 1 – Young's modulus of the composites at 25 °C; Modulus 2 – young's modulus of the composites at 90 °C.

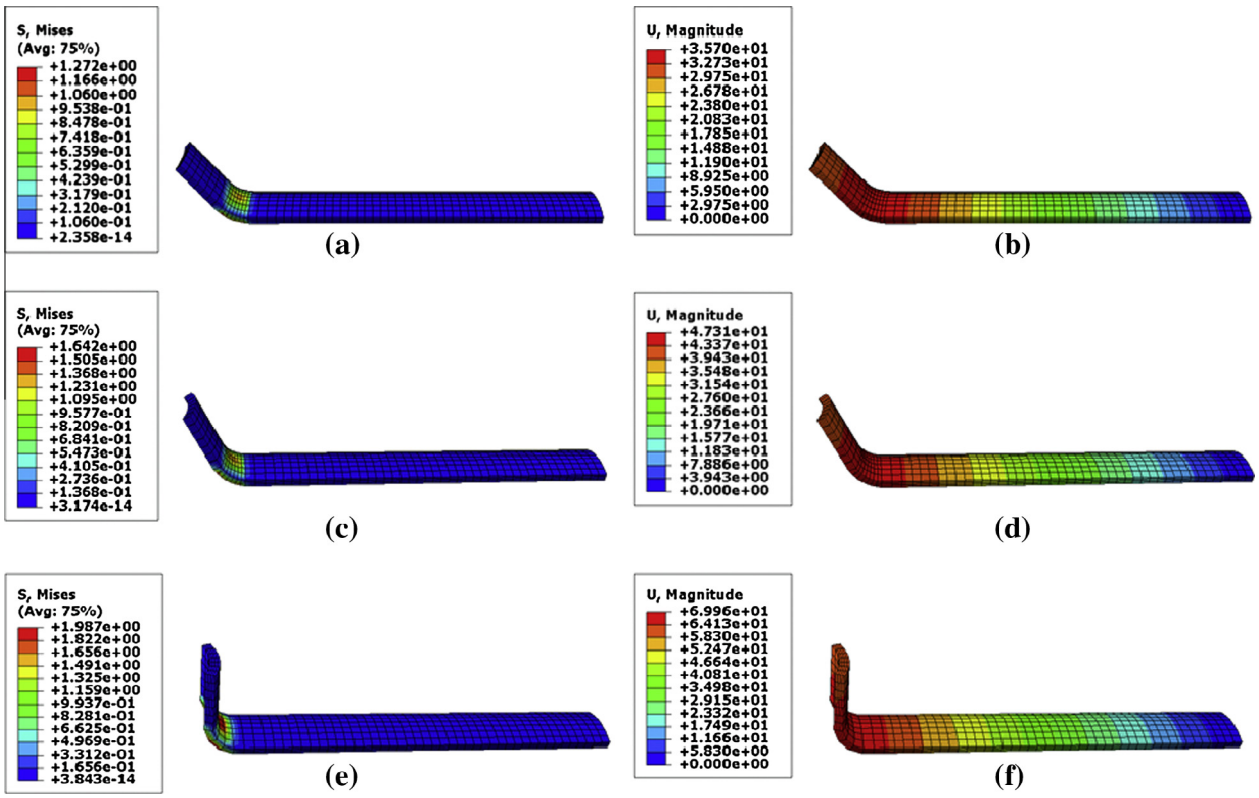

Fig. 6. (a) Mises stress distribution of laminate 1 in the "Lotus" device bent with 45°. (b) Displacement distribution of laminate 1 in the "Lotus" device bent with 45°. (c) Mises stress distribution of laminate 1 in the "Lotus" device bent with 60°. (d) Displacement distribution of laminate 1 in the "Lotus" device bent with 60°. (e) Mises stress distribution of laminate 1 in the "Lotus" device bent with 90°. (f) Displacement distribution of laminate 1 in the "Lotus" device bent with 90°.

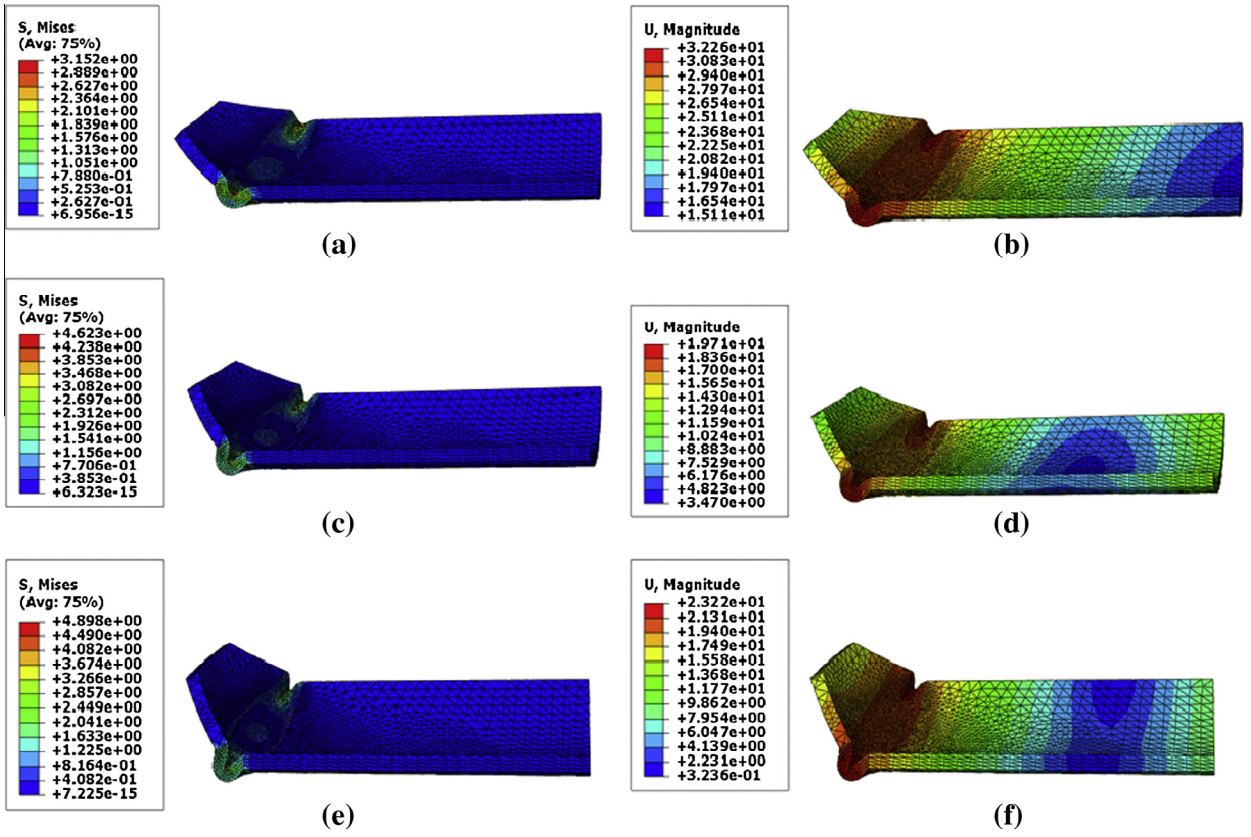

Fig. 7. (a) Mises stress distribution of laminate 2 in the "Lotus" device bent with 45°. (b) Displacement distribution of laminate 2 in the "Lotus" device bent with 45°. (c) Mises stress of distribution of laminate 2 in the "Lotus" device bent with 60°. (d) Displacement distribution of laminate 2 in the "Lotus" device bent with 60°. (e) Mises stress distribution of laminate 2 in the "Lotus" device bent with 65°. (f) Displacement distribution of laminate 2 in the "Lotus" device bent with 65°.

inside surfaces of the outer cylinder, 13.5 mm in length. Finally, the other end of the outer cylinder was fixed on the shelf. To facilitate the cylinders perfectly, the inner cylinder needed to bend outward (Fig. 3(c)); the outer cylinder needed to bend inward, as shown in Fig. 3(d). Finally, the two cylinders were installed as Fig. 3(e) shows. As long as one of the two cylinders deforms, the "Lotus" device will be released.

The "Eight paws" device uses the twisting deformation as the driving deployment [33]. Its parts are: 1-inner cylinder, 2-resistor heater, 3-eight-square octagon shaped deformable laminates, 4-laminate with an eight-square octagon hole, 5-outer cylinder. The fabrication of the "Eight paws" device is shown as follows: Firstly, one eight-square octagon shaped deformable laminate was fixed on the inner cylinder; meanwhile, another laminate with eight-square octagon hole was fixed on the outer cylinder, they were 10 mm in thickness. The hole is 1 mm bigger than the laminate on the inner cylinder, so the laminate can put into the hole easily (Fig. 4(a) and (b)). Secondly, the resistor heater was bonded to the inside surface of the inner cylinder, 20 mm in length. Thirdly, the inner cylinder was twisted 22.5° above *Tg* as the pre-deformation before connection. Then, the inner cylinder was put into the outer cylinder and the paws were twisted 22.5° to assemble the cylinders perfectly(Fig. 4(d)); eight barriers were bonded to the inside surface of the outer cylinder to make sure the paws cannot twist over 22.5°, as shown in Fig. 4(c) and (d). Finally, the other ends of the inner and outer cylinders were fixed on the shelves; the "Eight paws" device was assembled as Fig. 4(e) shows. When the instruction of release comes, the inner cylinder restores to its original shape upon heat, so as to drive the eight-square octagon shaped deformable laminates twists 22.5°.

Different from the smart release devices above, the "Bamboo" device was made of styrene, as shown in Fig. 5(d). It uses shrinking deformation to drive the release. The "Bamboo" device was built up with two similar stepped heat-shrinkable cylinders; each of the cylinders has two sections. The diameters increase by section presented in Fig. 5(a) and (b): 1-Third section, 2-Mating conical surface, 3-Fourth section, 4-First section, 5-Mating conical surface, 6-Second section (first section < second section < third section < fourth section). The inner diameter of the inner cylinder is 34 mm. To form the second section, it was expanded to 37 mm and the length of it is 40 mm; the last part of the first cylinder named first section. The outer cylinder was expanded to 42 mm at first, this section called third section, length 40 m; the last part of the outer cylinder was expanded to 44 mm to make the fourth section. Mating conical surfaces were formed after the expanding, which allows the cylinders to make an interference fit with each other, as shown in Fig. 5(c). The resistor heater was bonded on the inside surfaces of the second section. In order to make the inner

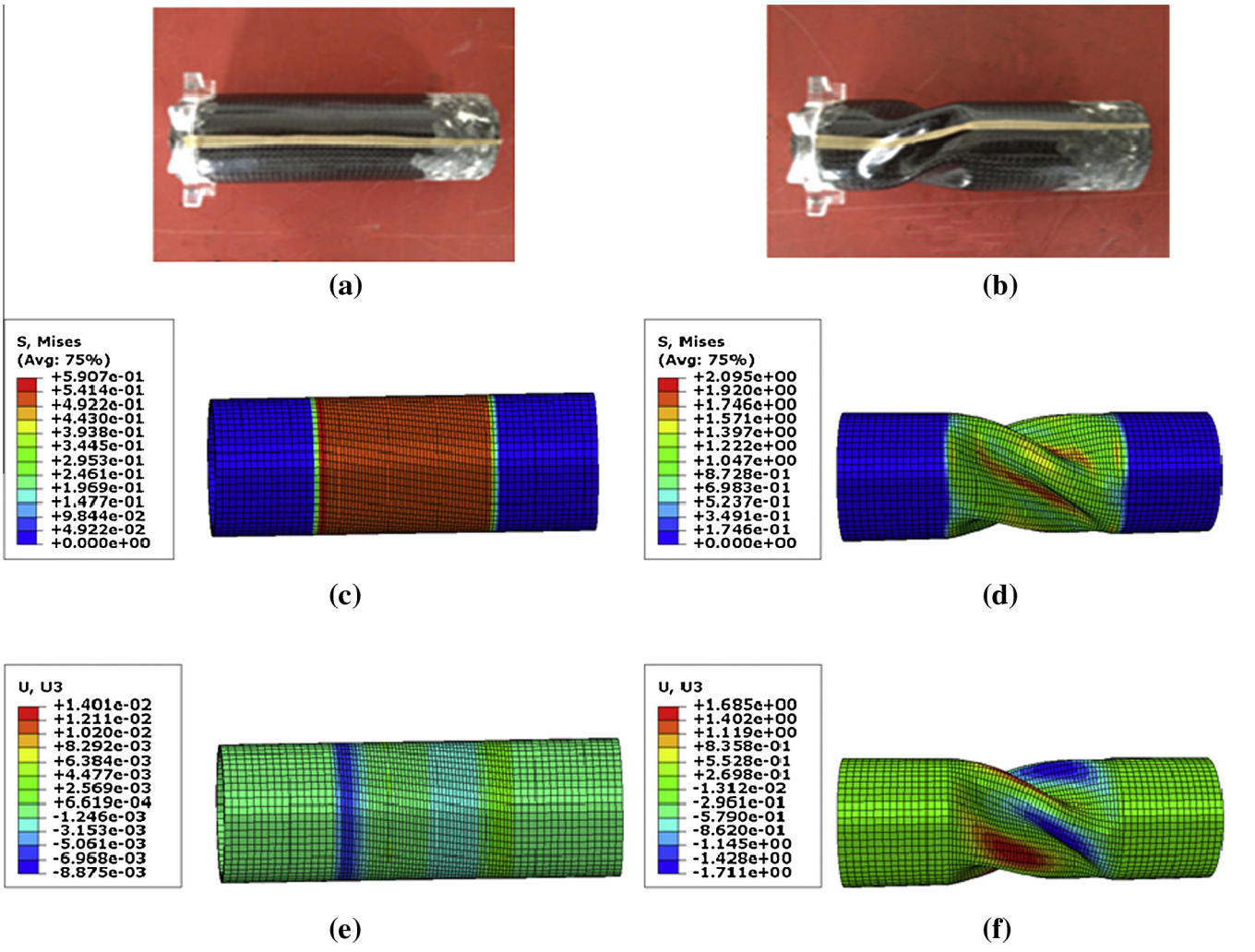

Fig. 8. (a) The inner cylinder of the "Eight paws" device. (b) The inner cylinder of the "Eight paws" device twisted with 60°. (c) Mises stress distribution of the inner cylinder in the "Eight paws" device twisted with 22.5°. (d) Mises stress distribution of the inner cylinder in the "Eight paws" device twisted with 60°. (e) Displacement distribution of the inner cylinder in the "Eight paws" device twisted with 22.5°. (f) Displacement distribution of the inner cylinder in the "Eight paws" device twisted with 60°.

and outer cylinders fit tightly, the "Bamboo" device was installed with a preload. When the instruction of release comes, the second section shrinks to 34 mm, and then the cylinders are separated. The advantage of this device is that it can be released stably in the vibration.

4. Model analysis

It is necessary to predict the distribution of stress and deformation to verify the feasibility of the smart release devices. In this work, analysis of the displacement and stress were applied by Abaqus 6.12 package.

According to the results of the tensile test of the materials, the material parameters of 4.92% carbon-fiber at 90 °C can be obtained in Table 3, Modulus of elasticity $E = 5.56$ MPa. Poisson's ratio $v = 0.35$. On the one hand, the simplified model of the inner cylinder named laminate 1 with the dimension of length 110 mm, thickness 2 mm, arc angle 45°, diameter 34 mm. The laminate 1 was bent with angle 45°, 60° and 90° outwards; Fig. 6 shows the maximum Mises stress are 1.272 MPa, 1.642 MPa, 1.987 MPa respectively, which concentrate on the middle of the bending part of laminate 1. On the other hand, the outer cylinder of the "Lotus" device was simplified as a deformable laminate named laminate 2, whose parameters are: length 70 mm, thickness 2 mm, arc angle 45°, diameter 66 mm. The laminate 2 were bent with 45°, 60° and 65° inwards presented in Fig. 7; On either side of the laminate 2 has a wrinkle, it increases gradually with the angle; Danger points concentrate on the two sides of the deforming part. Therefore, the six laminates break from their sides with excessive deformation.

The candidate part of the "Eight paws" device was simplified as a SMPC cylinder, whose parameters are: length 110 mm, thickness 2 mm, diameter 34 mm. Fig. 8(c)–(e) shows the part twisted with 22.5° and 60°, the maximum Mises stress of it is 0.59 MPa and 2 MPa respectively. It concentrated on the outer surface and the deformation was uniform when the cylinder was twisted 22.5°. Besides, the cylinder kept the shape of thin-wall tube until it was twisted 50°. However, when it was twisted 60°, an obvious wrinkle came out and stress state of the cylinder also changed, as shown in Fig. 8(d). The SMPC cylinder twists with 45° presented in Fig. 8(b), and it agrees with the model of the "Eight paws" device shown in Fig. 8(f). Consequently, the "Eight paws" device is feasible because it only needs to twist 22.5° for the release, and in this condition the inner cylinder keeps the shape of thin-wall tube.

Fig. 9 shows the "Bamboo" device was simplified as a deformable SMP cylinder with the dimension of length 110 mm, thickness 2 mm, diameter 34 mm. As shown in Table 3, Modulus of elasticity $E = 0.01$ MPa, Poisson's ratio $\underline{v} = 0.40$. In order to make the

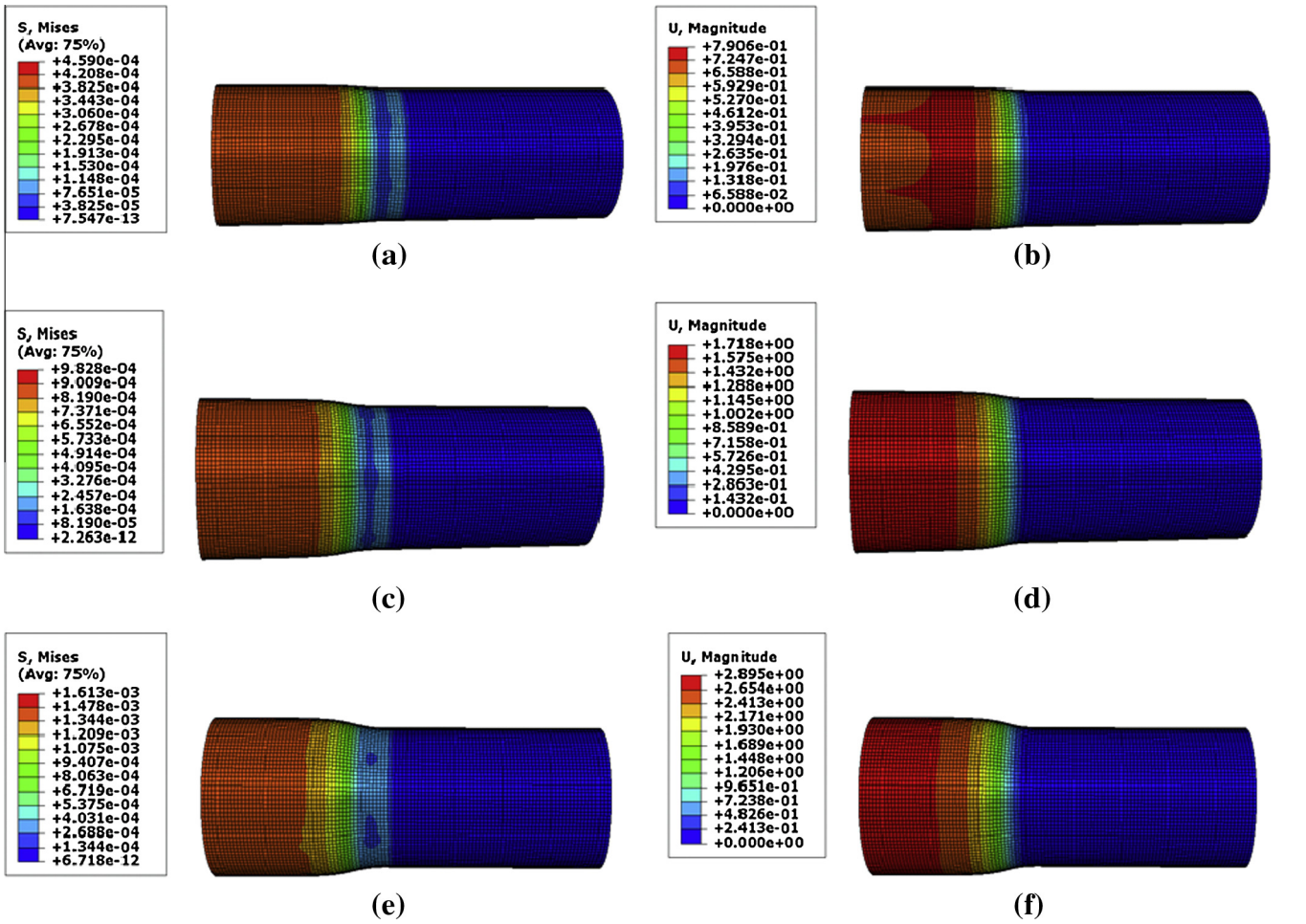

Fig. 9. (a) Mises stress distribution of the inner cylinder in the "Bamboo" device for a given parameter $P = 0.5 \times 10^{-4}$ MPa. (b) Displacement distribution of the inner cylinder in the "Bamboo" device for a given parameter $P = 0.5 \times 10^{-4}$ MPa. (c) Mises stress distribution of the inner cylinder in the "Bamboo" device for a given parameter $P = 1.0 \times 10^{-4}$ MPa. (d) Displacement distribution of the inner cylinder in the "Bamboo" device for a given parameter $P = 1.0 \times 10^{-4}$ MPa. (e) Mises stress distribution of the inner cylinder in the "Bamboo" device for a given parameter $P = 1.5 \times 10^{-4}$MPa. (f) Displacement distribution of the inner cylinder in the "Bamboo" device for a given parameter $P = 1.5 \times 10^{-4}$ MPa.

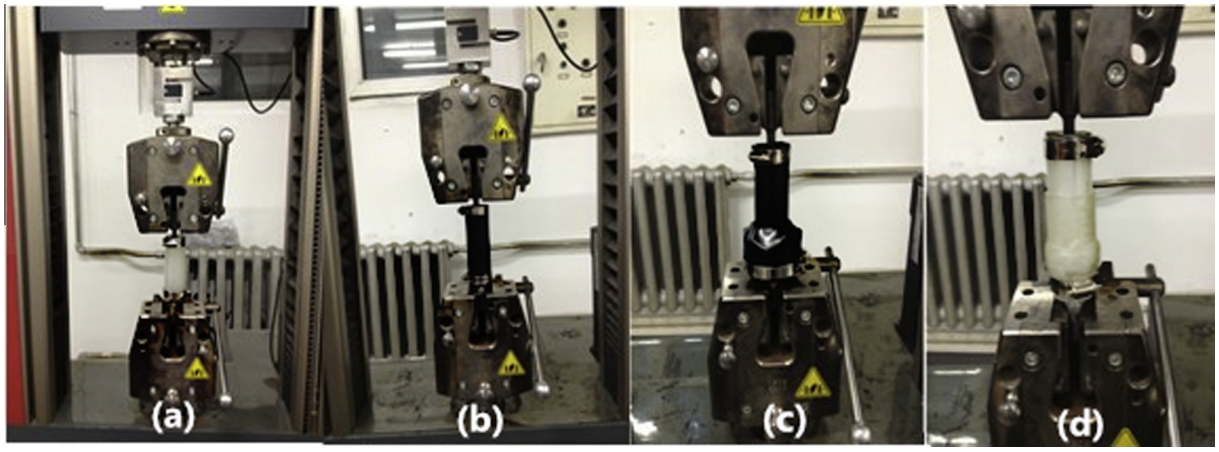

Fig. 10. (a) Tensile experiment of the SMP cylinder (b) Tensile experiment of the SMPC cylinder (c) Tensile experiment of the "Lotus" device (d) Tensile experiment of the "Bamboo" device.

"Bamboo" device, the diameter of the inner cylinder needs to increase 29.41%. For the pressure to expand the cylinders were not given, uniform pressure 0.5×10^{-4}MPa, 1.0×10^{-4}MPa and 1.5×10^{-4}MPa were set on the inner surface of the cylinder to simulate the deformation. The results shows that the maximum Mises stress are 4.6×10^{-4}MPa, 9.8×10^{-4}MPa and 0.2×10^{-4}MPa respectively. Fig. 9 shows the deformation distributes on the wall of the cylinder evenly, and its deformation agrees with the design of "Bamboo" device, as shown in Fig. 5(d).

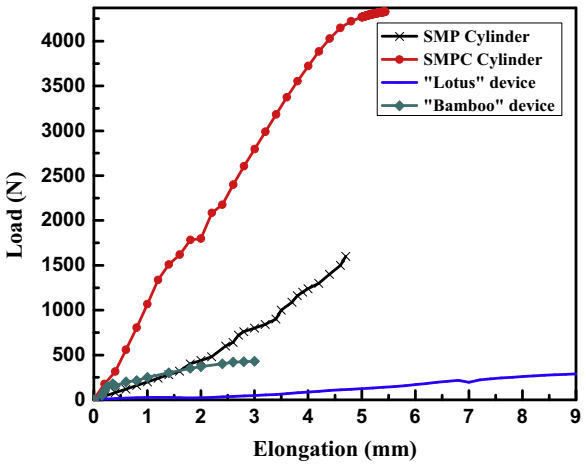

Fig. 11. Comparisons of Load-elongation relations of the SMP cylinder, SMPC cylinder, "Lotus" device and "Bamboo" device.

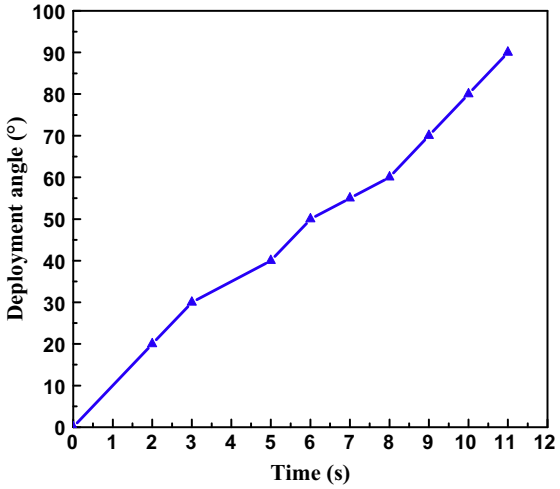

Fig. 13. Relations between bending angle and time of the "Lotus" device.

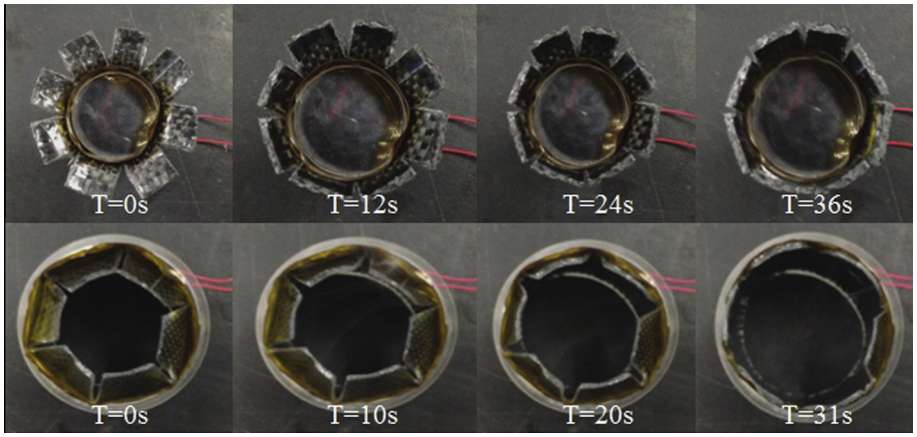

Fig. 12. Bending recovery tests of the inner and outer cylinder in the "lotus" device.

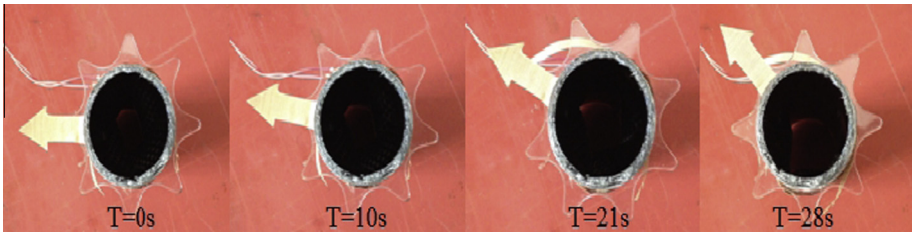

Fig. 14. Twisting recovery test of the SMPC cylinder.

5. Experimental verification

5.1. Tensile experiments of the smart release devices

As shown in Fig. 10, tensile experiment was conducted using ZWICK/Z010 with a loading rate of 2 mm/min. Fig. 11 shows the maximum loads of the SMP cylinder, the SMPC cylinder, the "Lotus" device and the "Bamboo" device are 1602.33 N, 4317 N, 284 N and 430 N, their elongation strains are 4.37%, 5.50%, 8.09%, 2.50%, respectively. The stress of SMPC cylinder is about 5 times than that of the SMP cylinder. When the elongation comes to 3 mm, the load of the "Bamboo" device is 430 N, almost 10 times of the "Bamboo" device.

In comparison of the three release device, the "Eight paws" device uses twisting deformation as the driving deployment, it needs to overcome friction to release and the paws of the "Eight paws" device cannot withstand too much load, so the "Bamboo" device has the largest structural strength from the design. The stability of the "Bamboo" device is the better than the "Lotus" device for its locking form is best.

5.2. Deformation recovery test of the smart release devices

From Fig. 12, the surfaces of the SMPC cylinders in the "Lotus" device are heated, and the inner cylinder needs 36 s to bend 90° outwards. The outer cylinder takes 31 s to bend 90° inwards. To release the "Lotus" device, the inner and outer cylinders were heated together and this makes the device has shorter release time. Because the inner and outer cylinders are separated before both of them bend to the original shape, thus the bending angel is less than 90°. Presuming the cylinders begin to deform when the temperature is above *Tg*, it takes 8 s to recover 60° and 11 s to bend 90°. The bending angle has a linear relationship with release time as Fig. 13 shows. The recovery experiment of the "Lotus" device was tested upon 15 N; both of the inner and outer cylinders are given 90° deformation; it takes 30 s to release even if the outer cylinder was cracked. To ensure the feasibility of the device, the bending angle should be set in 65° as the model analysis above shown.

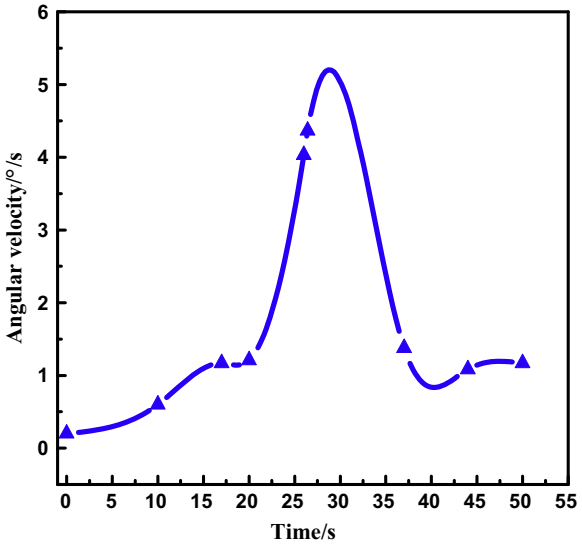

Fig. 16. Relations between twisting angular velocity and time of the "Eight paws" device.

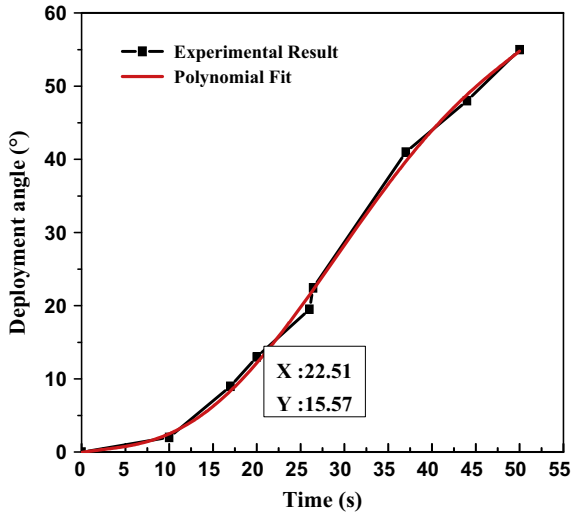

Fig. 15. Relations between twisting angle and time of the "Eight paws" device.

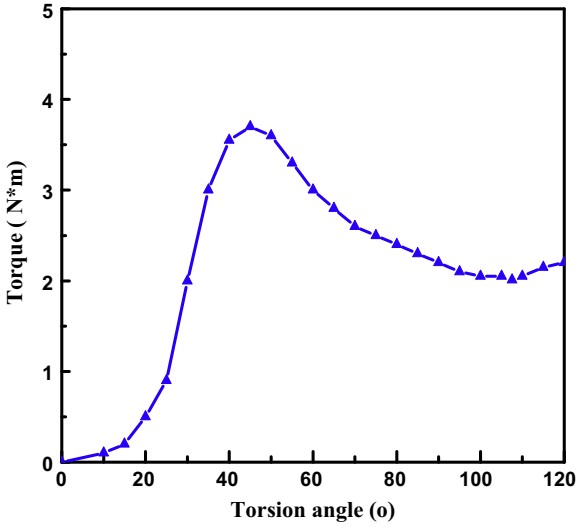

Fig. 17. Torque–angle relations of the "Eight paws" device.

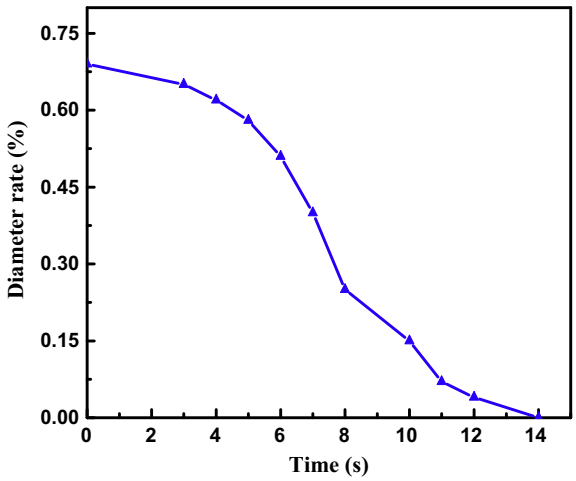

Fig. 18. Relations between diameter rate and time of the "Bamboo" device.

Table 4
Comparison of the smart release devices.

Characteristics	Lotus	Eight paws	Bamboo
Actuation time	8 s	15 s	7 s
Release time	30 s	26 s	30 s
Weight	82.03 g	88.03 g	43.73 g
Characters	Full release	Application of reverse deformation	Good release stability

From the twisting recovery test of the cylinder in the "Eight paws" device shown in Fig. 14, it takes 26 s to twist 22.5° quickly and smoothly for the SMPC cylinder. Presuming the cylinder begins to deform when the temperature is above *Tg*, the deforming time is about 15 s as shown in Fig. 15 [33]. When the time is 20 s, the angular velocity is 1.2 °/s. As shown in Fig. 16, there is a rapid increase and then the curve begins to decline after 30 s. From Torque–angle relations of the "Eight paws" device as Fig. 17 shows, the cylinder twists 22.5° with 0.6 N·m upon heat. The torque increases before 45°, it has a peak value with 45°, after that point the torque decreases.

In the recovery test of the "Bamboo" device in Fig. 18, it takes 14 s for the cylinder's diameter to decrease 69%. The "Bamboo" device spends 30 s to release upon 15 N. Presuming the smart release device begins to deform when the temperature is above *Tg*, the actuation time is 7 s. In summary, the three kinds of smart release devices have different characteristics shown in Table 4, therefore they are suitable for different occasions.

6. Conclusions

Three kinds of smart release devices, named "Lotus" device, "Eight paws" device and "Bamboo" device, have been designed and fabricated based on shape memory polymer composites. The total weights of them are 82.03 g, 88.03 g and 43.73 g. The resistor heater was applied to actuate the shape recovery process. The twisting, bending and shrinking deformations were used to drive deployment in the smart release devices respectively. Meanwhile, the displacement and stress of the smart release devices in different deformations have been simulated by model analysis to verify the feasible of the devices. Besides, the deformations of the smart release devices in the recovery experience agreed with that of the model analysis. The release time have been obtained by the recovery test, this time consist of the heating time and the actuation time. Through the comparison of the three release devices, the structural strength and release stability of "Bamboo" device is the best.

It has been found that the smart release devices are better than current release devices, because they are light weight, mechanically simple, low cost. Besides, these smart release devices can finish release upon load with no impacting shock, space debris and contamination. These conclusions and analysis are essential for many future applications which meet the needs of aerospace deployable mechanism to release the spacecraft. Next work will consider using filament winding process or pultrusion process to produce the smart release devices to achieve large carrying capabilities.

Acknowledgement

This work is supported by the National Natural Science Foundation of China (Grant Nos. 11225211, 11272106).

References

[1] Fosness E,Peffer A, Denoyer K. Overview of spacecraft deployment and release devices efforts at the Air Force Research Laboratory. In: 7th International conference and exposition on engineering, construction, operations, and business in space, Albuquerque, NM; 2000. p. 312–18.
[2] Leng J, Lan X, Liu Y, Du S. Shape-memory polymers and their composites: stimulus methods and applications. Mater Sci 2011;56(7):1077–135.
[3] Herbage E. Comparison of shape memory metals and polymers. Adv Eng Mater 2006;8:101–6.
[4] Huang W. On the selection of shape memory alloys for actuators. Mater Des 2002;23:11–9.
[5] Smith S, Dowen D, Fossness E, Peffer A. Development of shape memory alloy (SMA) actuated mechanisms for spacecraft release applications. In: 13th AIAA/USU conference on small satellites, Logan, UT, Paper No. SSC99-XI-7; 1999.
[6] Gall KR, Lake MS. Development of a shockless thermally actuated release nut using elastic memory composite material. In: 44th Structural dynamics, and materials conference, Norfolk, Virginia, Paper No. AIAA2003-1582; 2003.
[7] Sun J, Liu Y, Leng J. Mechanical properties of shape momery polymer composites enhanced by elastic fibers and their application in variable stiffness morphing skins. J Intel Mater Syst Struct 2014.
[8] Ji F, Zhu Y, Hu J, Liu Y, Yeung L, Ye G. Smart polymer fibers with shape memory effect. Smart Mater Struct 2006;15:1547–54.
[9] Liu Y, Gall K, Dunn M, McCluskey P. Thermo mechanics of shape memory polymer nanocomposites. Mech Mater 2004;36:929–40.
[10] Guo X, Liu L, Liu Y, Bo Z, Leng J. Constitutive model for a stress and thermal-induced phase transition in a shape memory polymer. Smart Mater Struct 2014;23:105019.
[11] Lv H, Yu K, Sun S, Liu Y, Leng J. Mechanical and shape memory behavior of shape memory polymer composites with hybrid fillers. Polym Int 2010;59:766–71.
[12] Wei Z, Sandstrom R, Miyazaki S. Shape memory materials and hybrid composites for smart systems-part II shape memory hybrid composites. J Mater Sci 1998;33:3763–83.
[13] Lu M, Tian Z, Tan H. Vibration and shape control of inflatable deployment structures. Proc SPIE 2007;6423:64235V.
[14] Keihl M, Bortolin R, Sanders B. Mechanical properties of shape memory polymers for morphing aircraft applications. Proceedings of SPIE smart structures and materials, industrial and commercial applications of smart structures technologies, San Diego, CA, 6 March, vol. 5762. Bellingham, WA: SPIE; 2005. p. 143–51.
[15] Perkins D, Reed J, Havens E. Morphing wing structures for loitering air vehicles. In: 45th AIAA/ASME/ ASCE/AHS/ASC structures, structural dynamics and materials conference, Palm Springs, CA, 19-22 April, AIAA 2004-1888. Reston, VA: AIAA; 2004.
[16] Basit A, Hostis G, Durand B. Multi-shape memory effect in shape memory polymer composites. Mater Lett 2012;74:220–2.
[17] Tan Q, Liu L, Liu Y. Thermal mechanical constitutive model of fiber reinforced shape memory polymer composite: based on bridging model. Compos A Appl Sci Manuf 2014;64:132–8.
[18] Yu K, Liu Y, Leng J. Shape memory polymer/CNT composites and their microwave induced shape memory behaviors. RSC Adv 2014;4:2961–8.
[19] Yu K, Westbrook K, Kao P. Design considerations for shape memory polymer composites with magnetic particles. J Compos Mater 2013;47:51–63.
[20] Zhang P, Li G. Structural relaxation behavior of strain hardened shape memory polymer fibers for self-healing applications. J Polym Sci, Part B: Polym Phys 2013;51:966–77.
[21] Ohki T, Ni Q, Ohsako N, Iwamoto M. Mechanical and shape memory behavior of composites with shape memory polymer. Compos A Appl Sci Manuf 2004;35(9):1065–73.

[22] Meng Q, Hu J. A review of shape memory polymer composites and blends. Compos A Appl Sci Manuf 2009;40:1661–72.
[23] Lan X, Liu Y, Lv H. Fiber reinforced shape memory polymer composite and its application in a deployable hinge. Smart Mater Struct 2009;18:024002.
[24] Liu C, Mater P. Polymers for shape memory applications. ANTEC Proc 2003:1962–6.
[25] Liu Y, Lv H, Lan X, Leng J, Du S. Review of electro-activate shape-memory polymer composite. Compos Sci Technol 2009;69(13):2064–8.
[26] Behl M, Lendlein A. Shape-memory polymers. Mater Today 2007;10(4):20–8.
[27] Ratna D, Karger-Kocsis J. Recent advances in shape memory polymers and composites: a review. J Nanosci Nanotechnol 2008;43:254–69.
[28] Liu Y, Du H, Liu L, Leng J. Shape memory polymer composites and their applications in aerospace: a review. Smart Mater Struct, 23023001; 2014.
[29] Wei Z, Sandstrom R, Miyazaki S. Shape-memory materials and hybrid composites for smart systems I. Shape-memory materials. J Mater Sci 1998:333743–62.
[30] Tan Q, Liu L, Liu Y, Leng J. Post buckling analysis of a shape memory polymer composite laminate with a built-in stiff film. Composites 2013:B53218–25.
[31] Liu Y, Gall K, Dunn M, Greenberg A, Diani J. Thermo mechanics of shape memory polymers: uniaxial experiments and constitutive modeling Int. J Plast 2006:22279–313.
[32] Mather P, Luo X, Rousseau I. Shape memory polymer research. Annu Rev Mater Res 2009:39445–71.
[33] Wei H, Guan C, Du H, Liu L, Leng J. A new release device based on styrene-based SMP reinforced by carbon fiber. In: Proc. SPIE 8793, Fourth International Conference on Smart Materials and Nanotechnology in Engineering, 2013; 87930C.